Assessing Existing Correlations and Proposing a New Heat Transfer Correlation for High-Pr Fluid Pebble Bed Reactors

By

Emma Scott

Submitted to the Department of Mechanical Engineering

in partial fulfillment of the requirements for the degree of

BACHELOR OF SCIENCE IN MECHANICAL ENGINEERING

at the

MASSACHUSETTS INSTITUTE OF TECHNOLOGY

May 2026

Authored by: Emma Scott
Mechanical Engineering
May 15, 2026

Certified by: Pierre Lermusiaux
Professor of Mechanical Engineering
Thesis supervisor

Accepted by: Daniel Frey
Professor of Mechanical Engineering
Undergraduate Officer

Assessing Existing Correlations and Proposing a New Heat Transfer Correlation for High-Pr Fluid Pebble Bed Reactors

by
Emma Scott

Submitted to the Department of Mechanical Engineering

in partial fulfillment of the requirements for the degree of

BACHELOR OF SCIENCE IN MECHANICAL ENGINEERING

Abstract

Fluoride-salt-cooled high-temperature reactors (FHRs) are a Gen IV nuclear reactor design that combine the meltdown resistance and online refueling capabilities of pebble-bed cores with the excellent heat transfer properties and atmospheric pressure operation of molten salt coolants. Accurate prediction of the convective heat transfer (directly determined by the Nusselt number) between fuel pebbles and the surrounding coolant is critical to both the safety and efficiency of these reactors. Many classical packed-bed Nusselt correlations widely used in reactor analysis codes (Wakao, KTA, Gunn, Gnielinski, Achenbach, Whitaker, and Petrovic) were developed almost entirely with gas-cooled data ($Pr \approx 0.7$), while FHR conditions involve molten salts with $Pr \approx 11–25$. Use of these correlations in FHR contexts extrapolates them well beyond their original calibration ranges, introducing uncertainty into reactor design tools at a critical stage of FHR development.

This thesis addresses that gap by analyzing a compiled dataset of high-Pr pebble-bed heat transfer results drawn from three experimental studies (Meng 2012, Liu 2018, Wang 2022) and four CFD studies (Dave 2020, Yuan 2023, Wang 2024, Liu 2025). The compiled dataset spans $Re \approx 50–6600$, $Pr \approx 6–24$, and porosities $\varepsilon \approx 0.26–0.57$. Seven classical correlations and four modern high-Pr correlations are benchmarked against each dataset using mean absolute relative error, with results grouped by porosity to expose porosity-dependent biases. The analysis reveals that correlations with explicit porosity dependence (KTA, Gnielinski, Gunn) systematically over-predict at low porosity due to extrapolation of their ε-dependent terms, while Achenbach consistently under-predicts due to its absence of a Pr term. Wakao demonstrates the most consistent behavior across porosity ranges.

A supplementary OpenFOAM single-sphere study evaluates the commonly cited thermal-boundary-layer-thinning argument for high-Pr discrepancies and finds that the argument does not directly extend to laminar single-sphere geometries. This suggests that packed-bed-specific transport mechanisms and configurations, rather than pure boundary-layer scaling, may be driving the observed differences in the packed-bed correlations.

A new correlation of the form $Nu = 4.08Re^{0.39}Pr^{0.4}$ is developed via ordinary least-squares regression in log-space across a selected subset of the compiled dataset (the high porosity cases were determined to be outliers and excluded from the fit). This correlation achieves the lowest mean error in the low and mid-porosity bins, which is the regime most relevant to FHR operation ($\varepsilon \approx 0.4$). The exponents are consistent with both the transition-regime Re scaling expected in the FHR-relevant Re range of 100–1000 and the high-Pr empirical scaling observed across independent fits in the literature. The proposed correlation may provide an improved tool for FHR thermal-hydraulic analysis within its calibration envelope and may serve as a benchmark for future correlation development as additional high-Pr pebble-bed data becomes available.

Thesis supervisor: Pierre Lermusiaux
Title: Professor of Mechanical Engineering

Acknowledgements

Thank you to Pierre Lermusiaux for guidance throughout the thesis process, particularly on how to sanity check my own fitting algorithms and giving me the knowledge required to run my own CFD studies. Also thank you to Abe Gertler at Kairos Power for helping me brainstorm an interesting and relevant Gen IV reactor problem to study.

Table of Contents

List of Figures

List of Tables

1. Introduction

1.1 Motivation

Gen IV nuclear reactors are increasingly gaining attention as a promising way to provide steady carbon-free energy. Nuclear power is a long-standing technology, but high construction costs and inability to follow demand like gas turbine technologies have made many reactors economically infeasible to continue operating [1]. Improved safety and lower cost of construction, combined with the recent uptick in demand for powering AI data centers, are all reasons for the pursuit of Gen IV reactors (as opposed to continuing with traditional designs).[2] [3] The Generation IV international forum was officially chartered in 2001 to review 100+ new reactor design concepts, and six were chosen as the most promising future designs by late 2002. These six were: gas-cooled fast reactor, lead-cooled fast reactor, molten salt reactor, sodium-cooled fast reactor, supercritical water-cooled reactor, and very high temperature gas reactor.[4]
In general, these designs are meant to increase efficiency and provide modularity, allowing for a smaller reactor that can be constructed faster, cheaper, and where it is needed. The two designs of focus for this study are molten salt and very high temperature reactors. Molten salt is being pursued as an advantageous heat transfer fluid for nuclear reactors because it can operate at high temperatures without pressurization (a difficult and costly aspect of traditional reactors). This allows for higher temperature operation and subsequently improved efficiency. Molten salt also offers improved heat transfer capabilities over water, is resistant to radiation, and cools to a contained solid if it were to react with surrounding air.[5] Salts are typically fluoride-based, with FLiBe (lithium tetrafluoroberyllate) being a commonly chosen option.

Very high temperature reactors include the pebble bed reactor (PBR), in which traditional fuel rods are replaced by thousands of fuel pebbles. Each of the pebbles contains tristructural isotropic (TRISO) uranium fuel particles surrounded by a layer of graphite that acts as the containment and moderation vessel of the radioactive material. This concept was first developed in West Germany in the 1960s (AVR reactor) and later leased to South Africa and China for development. Advantages of this design include online refueling capabilities, resistance to meltdown (due to the TRISO particles' high containment capabilities), and passive cooling capabilities (high volume to surface area capability and convection capability of the gas). Traditionally, this design has been used with gas (helium) because it is chemically inert, can be channeled directly into a Brayton cycle, and enables higher temperature operation (improved

[1] "Role of Natural Gas."
[2] "Generation IV Goals, Technologies and GIF R&D Roadmap | GIF Portal."
[3] IAEA, "Data Centres, Artificial Intelligence and Cryptocurrencies Eye Advanced Nuclear to Meet Growing Power Needs."
[4] "Generation IV Nuclear Reactors - World Nuclear Association."
[5] Khan, "Approval of Nuclear Pilot Plant That Uses Molten Salt Coolant Instead of Water a Step towards Safer Reactors," .

efficiency).[6] [7] However, gas is a poor heat transfer fluid compared to liquids. Due to this, fluoride salt cooled pebble bed reactor (FHR) designs are being pursued to combine the benefits of both designs. These designs are being actively pursued at various universities including the Shanghai Institute of Applied Physics, Xi'an University, UC Berkeley, as well as commercially by Kairos Power (Liu 2025)[8].

1.2 Definitions

$\dot{Q}$ = heat transfer rate h = convective heat transfer coefficient A = surface area k = thermal conductivity D = pebble diameter L = characteristic length μ = dynamic viscosity c_p = specific heat capacity ρ = density v = fluid velocity P = wetted perimeter E = porosity j_d = Chilton–Colburn mass-transfer j-factor α = molecular diffusivity υ_t = turbulent eddy viscosity Pr_t = turbulent Prandtl number α_t = turbulent thermal diffusivity $\alpha_{eff} = \alpha + \alpha_t$ = effective diffusivity q" = heat flux	Nu = Nusselt number = $\frac{hL}{k}$ Pr = Prandtl number = $\frac{\mu c_p}{k}$ Re = Reynolds number = $\frac{\rho v D}{\mu}$ PBR = pebble bed reactor TRISO = tristuctural isotropic uranium fuel particles FHR = fluoride salt cooled pebble bed reactor KP-FHR = Kairos power FHR HTGR = high temperature gas reactor HTS = heat transfer salt

Table 1: Compiled definitions and abbreviations used throughout the thesis

1.3 Nu relevance + High Pr Gap

Establishing the heat transfer rate from the pebbles to the fluid is critical for reactor design and operation, and is what determines both the safety and efficiency of the reactor. More heat generated by the fuel leads to higher power output; however, that heat must be removed fast enough for the reactor to avoid overheating and subsequent failure of the structural components of the reactor. The fluid flowing over the pebbles is forced convection, in which the heat transfer rate is described by Newton's Law:

[6] Energy.Gov, "X-Energy Is Developing a Pebble Bed Reactor That They Say Can't Melt Down."
[7] *Wikipedia*, "Pebble-bed reactor."
[8] Liu et al., "Numerical Research of Flow and Heat Transfer Characteristics of High-Prandtl-Number Fluoride Salt in the Pebble Bed Channel," November 2025.

$$\dot{Q} = hA\Delta T$$

where h is the convection heat transfer coefficient, A is the surface area, and ΔT is the temperature difference between the fluid and the pebbles. The value of h is determined by the following relation:

$$h = \frac{kNu}{L}$$

where k is the thermal conductivity, Nu is the Nusselt number (ratio of convective to conductive heat transfer), and L is the characteristic length, which in the case of pebble bed reactors is typically the pebble diameter D. Nu is determined by empirical correlations and depends on both the Prandtl number (Pr) and the Reynolds number (Re). $\text{Pr} = \frac{\mu c_p}{k}$ and $\text{Re} = \frac{\rho v D}{\mu}$, where μ is the dynamic viscosity, c_p is the specific heat capacity, D is the pebble diameter, ρ is the density, and v is the fluid velocity. Note that some definitions of Re in the literature are the hydraulic diameter, which involves a porosity (ε) adjustment. To keep everything in the same terms for comparison purposes, all correlations will be expressed in terms of Re, with ε adjustments as specified.

The Pr of gases is ~0.7, and the operating Re range of helium-cooled PBRs is $O(10^5)$. For FHR conditions, Pr ~11-19 and Re range is $O(10^2 - 10^3)$. Classic correlations were developed using gas conditions, so efforts to utilize these relations for molten salt extrapolate them well beyond their original intended ranges and gas conditions (Dave, 2019)[9]. These correlations are often used as the basis for simulation codes. Some examples include Kairos Power using the Wakao correlation in their STAR-CCM+ codes[10], Argonne National Lab using KTA, Wakao, and Achenbach (to address wall effects) in their SAM code[11], and Idaho National Labs using the Petrovic correlation via the Pronghorn code[12]. Due to the importance of Nu on h, and subsequently on the reactor design, an accurate correlation is useful to both improve the accuracy of existing simulation tools and allow for higher confidence in the early stage design decisions where the cost of CFD or experiments may be prohibitively expensive.

1.4 Thesis Objectives

This thesis addresses the gap between the operating conditions of FHRs and the calibration range of available packed-bed Nu correlations. The classical correlations were developed almost exclusively at Pr ≈ 0.7, while FHR conditions involve Pr ≈ 11–25 and Re ≈ 100–1000. The

[9] Dave et al., "Numerical Assessment of Packed-Bed Heat Transfer Correlations for Molten Salt."
[10] Kairos Power; "KP-FHR Core Design and Analysis Methodology Topical Report."
[11] Hu et al., *Development of a Reference Model for Molten-Salt-Cooled Pebble-Bed Reactor Using SAM*.
[12] Ortensi et al., *Fluoride-Cooled High-Temperature Pebble-Bed Reactor Reference Plant Model*.

extrapolation introduces uncertainty into the reactor analysis codes that rely on these correlations. The present work seeks to achieve four objectives:

1. Compile a unified high-Pr pebble-bed dataset spanning Pr ≈ 6–24, drawn from both physical experiments and CFD studies. Data is presented both as is and in consolidated forms (presented with porosity scaling and Pr collapsed plots) to enable direct cross-study comparison as available.
2. Benchmark the major classical correlations (Whitaker, Gunn, Wakao, KTA, Achenbach, Gnielinski, Petrovic) and the modern high-Pr correlations (Meng, Liu, Wang) against each dataset using mean absolute relative error. Results will be stratified by porosity to examine any porosity-dependent biases. From this analysis, recommendations are provided regarding which correlations are most appropriate in a range of physical scenarios.
3. Examine the physical reasoning commonly invoked to explain the gas-to-salt discrepancy, particularly the thermal-boundary-layer-thinning argument presented by several authors, through a supplementary single-sphere OpenFOAM study comparing air, water, and FLiBe at matched Re. The aim is to investigate whether the claimed mechanism explains the observed errors or whether packed-bed-specific physics is more likely the dominant cause.
4. Develop a new correlation calibrated specifically to high-Pr packed-bed conditions, compare its performance against existing correlations, and establish its limitations and validity range. The intent is not to derive a mechanistically novel form, but to provide an empirically grounded and improved reference specifically for FHR-relevant conditions to supplement the existing literature.

Together, these objectives aim to move FHR heat transfer analysis from reliance on the gas-cooled correlations toward a calibrated, high-Pr specific basis suitable for use in reactor design decisions.

2. Background

2.1 FLiBe and FHR operating conditions

The relevant thermophysical properties of FLiBe for the typical operating conditions of an FHR are as follows (c_p = 2397.73 ($\frac{J}{kg \cdot K}$) and k = 1 ($\frac{W}{m \cdot K}$) are given as constant values):

T (℃)	μ ($\cdot 10^3$)	ρ	Pr
550	11.1	2011	26.6
600	8.5	1987	20.5
650	6.8	1962	16.2
700	5.5	1938	13.1

Table 2: Thermophysical properties at operating temperatures relevant to FHRs. Data taken from INL thermophysical properties handbook.

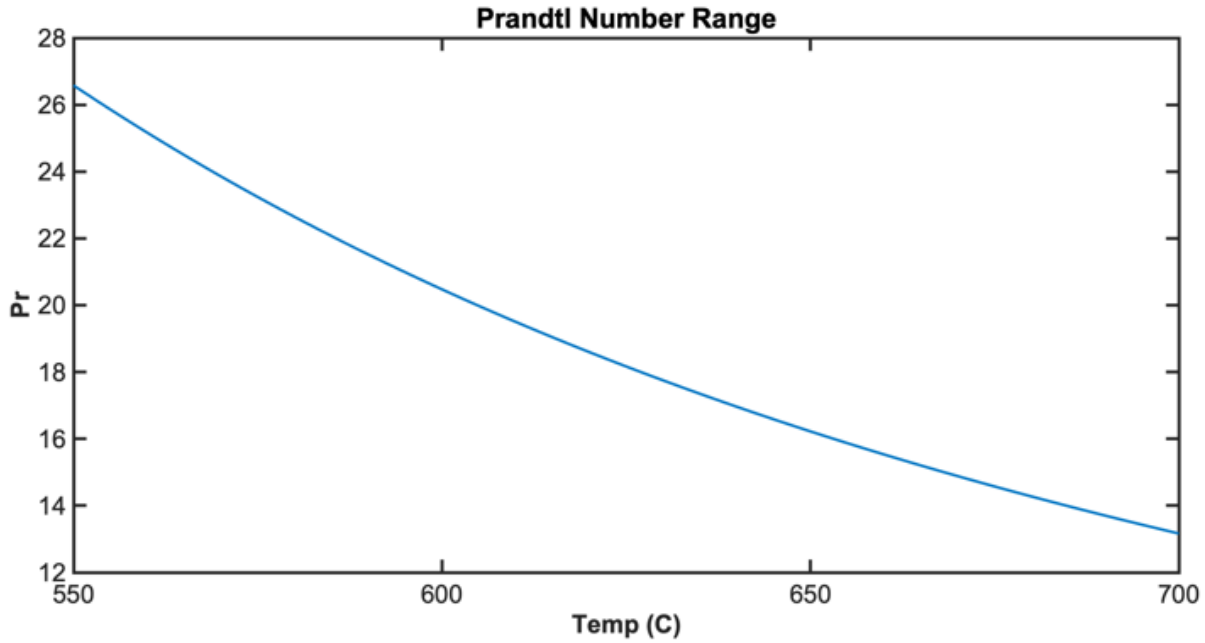

Figure 1: Pr range across T = 550-700C.

The documented temperature range in the KP-FHR source documentation[10] is 550-650 °C. This temperature envelope (+50 ℃ for margin) is presented to justify the Pr range of 14-25, representing the majority of FLiBe conditions in the PBR.

The Re is affected by fluid properties (density and dynamic viscosity), as well as the velocity of flow and pebble diameter. The velocity varies from the inlet to the outlet of the pebble bed and changes over the course of the tortuous flow it follows. This, in addition to the changing physical properties with temperature (table 1), accounts for the Re variation across the FHR. The pebble diameter ranges from 8mm (Liu 2024) to 60mm (Wang 2024)[13]. The Kairos documentation gives a reference value of 40mm diameter.[12] The varying diameters are another reason for the wide

[13] Wang et al., "Numerical Analysis and Validation on Heat Transfer Characteristics and Correlation of Molten Salt in Pebble Bed Channel."

range of Re presented across experimental/simulation studies. The typical porosity of randomly packed pebble beds is ~0.36-0.4.

2.2 Existing relevant correlations

The following 7 correlations form the comparison set against which CFD results and experimental data are commonly benchmarked in pebble-bed thermal-hydraulics. These 7 were chosen for their historical significance, use in reference codes and documentation, as well as prevalence in the literature.

1. **Whitaker (1972)**[14]: $\mathrm{Nu} = \left(\left(0.5\frac{Re^{\frac{1}{2}}}{1-\varepsilon} + 0.2\frac{Re^{\frac{2}{3}}}{1-\varepsilon}\right)Pr^{\frac{1}{3}}\right)\cdot\frac{1-\varepsilon}{\varepsilon}$

   Intended ranges: $\mathrm{Re}/(1-\varepsilon) = 20–8{,}000$, $\varepsilon = 0.34–0.78$, $\mathrm{Pr} \approx 0.6–0.7$

   Whitaker's correlation was derived as a unifying correlation across pipes, flat plates, single cylinders, single spheres, packed beds, and staggered tube bundles by compiling forty years of forced-convection data. He showed that one functional form fit randomly packed beds of spheres, cylinders, Raschig rings, partition rings, and Berl saddles to within ±25%. It is the broadest-geometry correlation in the set. Whitaker notes it is not meant to be highly accurate for a specific case but is meant to be useful for broad design problems.

2. **Gunn (1978)**[15]: $\mathrm{Nu} = (7 - 10\varepsilon + 5\varepsilon^2)(1 + 0.7Re^{\frac{1}{2}}Pr^{\frac{1}{3}}) + (1.33 - 2.4\varepsilon + 1.2\varepsilon^2)Re^{0.7}Pr^{\frac{1}{3}}$

   Intended ranges: $\mathrm{Re} = 10–10^5$, $\varepsilon \geq 0.35$, $\mathrm{Pr} \approx 0.7$.

   Gunn's correlation was created for use on randomly packed beds of spheres in fixed and fluidized configurations. Gunn built the correlation to satisfy four asymptotic limits — single-particle and packed-bed behavior at both low and high Re — and explicitly embedded an ε-dependence. This is the only correlation in the set with explicit quadratic porosity terms in both the low- and high-Re branches.

[14] Whitaker, "Forced Convection Heat Transfer Correlations for Flow in Pipes, Past Flat Plates, Single Cylinders, Single Spheres, and for Flow in Packed Beds and Tube Bundles."
[15] Gunn, "Transfer of Heat or Mass to Particles in Fixed and Fluidised Beds."

3. **Wakao & Kaguei (1979)[16]**: Nu = $2 + 1.1Re^{0.6}Pr^{\frac{1}{3}}$

   Intended ranges: Re = 15–8,500, ε ≈ 0.4, Pr ≈ 0.7.

   Wakao's correlation is intended for use in describing randomly packed beds of spheres, with the original data on which the fit was based corrected for axial fluid thermal dispersion. It was derived directly from a previous analogous mass-transfer correlation by Wakao and Funazkri, leading to the $Pr^{\frac{1}{3}}$ term. The dataset behind it spans 13+ studies recomputed under a corrected dispersion-coefficient model. It is one of the most widely used packed-bed Nu correlations.

4. **KTA (1983)[17]**: Nu = $\frac{1.27Pr^{\frac{1}{3}}Re^{0.36}}{\varepsilon^{1.18}} + \frac{0.033Pr^{0.5}Re^{0.86}}{\varepsilon^{1.07}}$

   Intended ranges: Re = 100–10^5, Pr ≈ 0.7, ε = 0.36–0.42.

   Geometric requirements: $\frac{D_{bed}}{D_{pebble}} > 20$ and H > $4D_{pebble}$ (conditions that are easily met by a typical FHR design).

   The KTA correlation is intended for use in describing randomly packed spherical fuel elements in HTGR cores cooled by helium gas. The KTA standard is a calibrated nuclear safety correlation built from independent helium pebble-bed studies and certified by the German Nuclear Safety Standards Commission for HTGR core design. It is one of the most common reference correlations in nuclear codes (ex. SAM) because of its regulatory status, but the original dataset is not publicly documented.

5. **Achenbach (1995)[18]**: Nu = $((1.18Re^{0.58})^4 + (0.23\frac{Re}{1-\varepsilon}^{0.75})^4)^{\frac{1}{4}}$

   Intended ranges: Re/ε up to 7.7×10^5, Pr ≈ 0.71, ε = 0.387.

   Achenbach's correlation is based on experimental data. In his experiment, a single 60 mm copper test sphere was buried in a randomly packed graphite bed (D_{bed} = 0.983 m, H = 0.84 m) and measured to determine the heat transfer properties. This was done with air and was intended to get heat transfer data for higher Re numbers than previously

[16] Wakao, *FLUID DISPERSION COEFFICIENTS ON PARTICLE-TO-FLUID HEAT TRANSFER COEFFICIENTS IN PACKED BEDS*.
[17] *KTA 3102.2 Reactor Core Design of High-Temperature Gas-Cooled Reactors; Part 2: Heat Transfer in Spherical Fuel Elements*.
[18] "Achenbach- Heat and Flow Characteristics of Packed Beds."

recorded. It is a common reference for high-Re randomly packed beds with air, but its lack of a Pr term leads to higher error when used for other fluids.

6. **Gnielinski (1978)**: Nu = $(2 + (Nu_l^2 + Nu_t^2)^{\frac{1}{2}})(1 + 1.5(1-\varepsilon))$

$$Nu_l = 0.664 Pr^{\frac{1}{3}} \left(\frac{Re}{\varepsilon}\right)^{\frac{1}{2}} \qquad Nu_t = \frac{0.037 Pr \left(\frac{Re}{\varepsilon}\right)^{0.8}}{1+2.443\left(\frac{Re}{\varepsilon}\right)^{-0.1}\left(Pr^{\frac{2}{3}}-1\right)}$$

Original range: $\frac{\mathrm{Re}}{\varepsilon} \approx 1–2\times10^4$, $0.26 \leq \varepsilon \leq 0.935$, Pr 0.7-$10^4$

Gnielinski's correlation was developed using a semi-empirical "single sphere + arrangement factor" strategy, rather than fitting data directly. He first built the single-sphere Nusselt number from three physical asymptotes: the conduction limit (Nu = 2 as Re → 0), a laminar flat-plate term ($Nu_l \propto Pr^{\frac{1}{3}}\left(\frac{Re}{\varepsilon}\right)^{\frac{1}{2}}$), and a turbulent boundary-layer term ($Nu_t \propto \mathrm{Re}^{0.8}\,\mathrm{Pr}$). To extend this to a randomly packed bed, he multiplied by an empirical arrangement factor $f(\varepsilon) = 1 + 1.5(1-\varepsilon)$, which helps represent the heat-transfer enhancement from neighboring pebbles squeezing the flow. The constants were calibrated against the combined experimental database of roughly 20 prior authors conducting heat transfer experiments. However, almost all the data it was validated on in the study was using Pr ≈ 0.7, hence the lack of confidence in using it for high Pr values. Note that the original source was not able to be found in English, so the form and description is taken from Wu (2025)[19].

7. **Petrovic and Thodos (1967)/Pronghorn Manual[20]:** Nu = $\frac{0.357 Pr^{\frac{1}{3}} Re^{0.641}}{\varepsilon}$

Original range: Re = 3–230, $0.395 \leq \varepsilon \leq 0.475$, $0.6 \leq \mathrm{Pr} \leq 5.5$

Petrovic's correlation was performed as a mass transfer experiment, vaporizing water and hydrocarbons from porous spheres in air. Their original result yielded $\varepsilon j_d = 0.357/\mathrm{Re}^{0.359}$ where j_d = the Chilton–Colburn mass-transfer j-factor. The Pronghorn Theory manual from INL uses the form Nu = $\frac{0.357 Pr^{\frac{1}{3}} Re^{0.641}}{\varepsilon}$, which follows the Chilton–Colburn substitution $j_d = j_h$ and algebraic rearrangement (a similar procedure is followed in Wakao's paper).

[19] Wu and Hibiki, "Particle-Fluid Heat Transfer for Laminar and Turbulent Flows in Packed Beds of Spherical Particles."
[20] "Pronghorn Theory Manual."

Correlation	Equation	Pr	Re	ε
Whitaker	$\text{Nu} = \left(\left(0.5\frac{Re^{\frac{1}{2}}}{1-\varepsilon} + 0.2\frac{Re^{\frac{2}{3}}}{1-\varepsilon}\right)Pr^{\frac{1}{3}}\right)\cdot\frac{1-\varepsilon}{\varepsilon}$	0.6–0.7	$(20 - 8{,}000)\cdot(1-\varepsilon)$	0.34–0.78
Gunn	$\text{Nu} = (7 - 10\varepsilon + 5\varepsilon^2)(1 + 0.7Re^{\frac{1}{2}}Pr^{\frac{1}{3}}) + (1.33 - 2.4\varepsilon + 1.2\varepsilon^2)Re^{0.7}Pr^{\frac{1}{3}}$	0.7	$10–10^5$	≥ 0.35
Wakao	$\text{Nu} = 2 + 1.1Re^{0.6}Pr^{\frac{1}{3}}$	0.7	15–8,500	0.4
KTA	$\text{Nu} = \frac{1.27Pr^{\frac{1}{3}}Re^{0.36}}{\varepsilon^{1.18}} + \frac{0.033Pr^{0.5}Re^{0.86}}{\varepsilon^{1.07}}$	0.7	$100–10^5$	0.36–0.42
Achenbach	$\text{Nu} = ((1.18Re^{0.58})^4 + (0.23\frac{Re}{1-\varepsilon}^{0.75})^4)^{\frac{1}{4}}$	0.71	$<(7.7\times10^5)\cdot\varepsilon$	0.387
Gnielinski	$\text{Nu} = (2 + (Nu_l^2 + Nu_t^2)^{\frac{1}{2}})(1 + 1.5(1-\varepsilon))$ $Nu_l = 0.664Pr^{\frac{1}{3}}(\frac{Re}{\varepsilon})^{\frac{1}{2}}$ $Nu_t = \frac{0.037Pr(\frac{Re}{\varepsilon})^{0.8}}{1+2.443(\frac{Re}{\varepsilon})^{-0.1}(Pr^{\frac{2}{3}}-1)}$	0.7–10^4	$(1-2\times10^4)\cdot\varepsilon$	0.26-0.935
Petrovic	$\text{Nu} = \frac{0.357Pr^{\frac{1}{3}}Re^{0.641}}{\varepsilon}$	0.6-5.5	3-230	$0.395 \le \varepsilon \le 0.475$

Table 3: Summary of the 7 classic correlations

2.3 Summary of 3 high Pr pebble bed heat transfer experiments

1. **Meng et al (2012)[21]**: This experiment was not explicitly for molten salt conditions but was conducted to provide higher Pr heat transfer data for PBR applications than was currently available (mostly Pr≈0.7). PBR conditions were simulated using distilled water as the working fluid and electromagnetic induction heated carbon steel spheres as the randomly packed pebbles. It was encased in a 75 mm ID × 980 mm crystal glass tube. Multiple tests were run with pebble diameters of 3mm and 8mm, inlet temperatures varying from 25-50℃, Pr = 2.6-5.7, Re = 1175-13069 and ε = 0.38. The relevant data used in this analysis was taken from a specific test with D=8mm, T= 25.3℃. A separate property reference sheet states Pr = 6.13 at T= 25.3℃ for water, but Meng reports the

[21] Meng et al., "Single-Phase Convection Heat Transfer Characteristics of Pebble-Bed Channels with Internal Heat Generation."

highest Pr as 5.7. For consistency with the author, Pr = 5.7 will be used in subsequent analysis. Meng fit a correlation to the data of the following form:

$$\text{Nu} = 3.212\left(\frac{\varepsilon Re}{1-\varepsilon}\right)^{0.335} Pr^{0.438}$$

The author provides little comparison to other correlations, except that Whitaker matches the data well when Nu is divided by $Pr^{\frac{1}{4}}$. This result was not able to be replicated in subsequent analysis, and instead found that Whitaker greatly overpredicts. Meng does not clearly define whether the conversion in their work is $Re_h = \frac{Re_d}{(1-\varepsilon)}$ (standard, explained in section 2.5) or $Re_h = \frac{\varepsilon Re_d}{(1-\varepsilon)}$. Plotting both, the data and correlation overlapped for the latter and did not for the former, so the first convention is used (consistent with the rest of the literature).

2. **Liu et al (2018)[22]**: FHR conditions were simulated using Dowtherm A thermal oil as FLiBe substitute (similar Pr), and electromagnetic induction heated carbon steel pebbles as fuel substitute. Two tests were run with pebble diameters of 8mm and 10mm, and varying inlet temperatures. The relevant data used in subsequent analysis was taken from a specific test at 67℃. The Dowtherm A thermal oil data sheet provides values at 65℃ which results in Pr = 20.5. For the experimental conditions, Re = 57-1576 and ε = 0.361-0.377. Liu fit a correlation to the data of the following form:

$$\text{Nu} = \left(\frac{0.0014}{\varepsilon^{5.99}}\left(\frac{Re}{1-\varepsilon}\right)^{0.76} Pr^{\frac{1}{4}}\right)\left(\frac{1-\varepsilon}{\varepsilon}\right) \quad \text{Re} \leq 170 \text{ and } \quad \text{Nu} = \left(\frac{0.0299}{\varepsilon^{4}}\left(\frac{Re}{1-\varepsilon}\right)^{0.56} Pr^{\frac{1}{4}}\right)\left(\frac{1-\varepsilon}{\varepsilon}\right) \quad \text{Re} > 170$$

They found that Wakao underpredicted by 45-60%, and KTA matched within 10% at low Re and 15-25% for higher Re (KTA underpredicted the data). They attribute the Wakao underprediction to the lack of porosity term in the equation since they use ε = 0.361-0.377 and ε = 0.4 was the intended porosity. They also state that KTA matches well because it does account for porosity. They also attribute the Meng underprediction to the fact that the authors used the center pebble temperature as the surface temperature, leading to the shallower slope (i.e. strong underprediction) of the correlation line. The authors reason that the difference in data vs correlation is due to a difference in the heat transfer mechanisms that the increased momentum to thermal boundary layer ratio induces. Since the thermal boundary layer is thinner, heat transfer is dominated by momentum diffusivity at the boundary layer.

[22] Liu et al., "Experimental Investigation of Flow and Convective Heat Transfer on a High-Prandtl-Number Fluid through the Nuclear Reactor Pebble Bed Core."

3. **Wang et al (2022)[23]**: FHR conditions were simulated using Heat Transfer Salt (HTS) and 60mm diameter graphite pebbles (heated by induction) encased in a SiC tube. This experiment was a single string of pebbles (as opposed to a randomly packed bed), leading to a very high ε = 0.5685. Inlet temperatures varied from 262-302℃, Re = 2800-6600, and Pr = 11.27-14.51. The relevant data used in this analysis was taken from a specific test at 262℃ (Pr = 14.51). Wang fit a correlation to the data of the following form:

   $\text{Nu} = 0.693 Re^{0.6} Pr^{0.392}$

   Wang found that KTA overpredicts by ~31% and Wakao overpredicts by ~27%. Meng is ~41% lower, Gnielinski is ~38% lower, and Whitaker provides the best estimate at ~10% below the data. Their defined Gnielinski correlation did not include the packed bed multiplication factor and therefore was cited as an underprediction. With the multiplication factor, Gnielinski actually matches very well (Figure 3). They explain the discrepancies by citing their high ε value (single row does not transfer heat as well as random bed, thus why KTA and Wakao are over, and Meng and Gnielinski have strong ε dependence). Whitaker cites in his work that his correlation performs better with regular arrangements (vs random), and Wang cites this as the reason for its success with their data.

Experiment	Fluid	Re	Pr	ε	d_p	Correlation
Meng (2012)	Water	1175-13069	2.6-5.7, calculated up to 6.13	0.38	3mm, 8mm	$\text{Nu} = 3.212(\frac{\varepsilon Re}{1-\varepsilon})^{0.335} Pr^{0.438}$
Liu (2018)	Dowtherm A Oil	57-1576	14-19 (listed), calculated up to 20.5	0.361–0.377	8mm, 10 mm	$\text{Nu} = (\frac{0.0014}{\varepsilon^{5.99}}(\frac{Re}{1-\varepsilon})^{0.76} Pr^{\frac{1}{4}})(\frac{1-\varepsilon}{\varepsilon})$ Re ≤ 170 $\text{Nu} = (\frac{0.0299}{\varepsilon^{4}}(\frac{Re}{1-\varepsilon})^{0.56} Pr^{\frac{1}{4}})(\frac{1-\varepsilon}{\varepsilon})$ Re > 170
Wang (2022)	HTS Molten Salt	2800-6600	11.27-14.51	0.5685	60mm	$\text{Nu} = 0.693 Re^{0.6} Pr^{0.392}$

Table 4: Summary of the 3 physical experimental datasets

2.4 Summary of 4 High Pr CFD Simulations

1. **Dave et al. (2020)[9]**: Dave performed CFD simulations of molten 2LiF–BeF_2 (FLiBe) flow through structured pebble lattices including both body-centered cubic (BCC), and face-centered cubic (FCC) arrangements. Dave used STAR-CCM+ with both k_ε (RANS)

[23] Wang et al., "Experimental Research on Convective Heat Transfer Characteristics of Molten Salt in a Pebble Bed Channel with Internal Heat Source."

and Large Eddy Simulation (LES) turbulence models (k_ε is reported for subsequent analysis as it had significantly more data points, and the LES vs k_ε values were not significantly different from each other). The study spanned Re = 100-2250, Pr≈16, and ε = 0.26 (FCC), and 0.32 (BCC).

The authors compared their data against multiple existing correlations (Wakao, Gnielinski, KTA, Meng) and found that most failed to capture the qualitative trend. They found that the Meng correlation gave the best agreement at $3\times10^2 < Re < 2\times10^3$; however, their reported form of the Meng equation uses the Reynolds number $Re * \frac{1-\varepsilon}{\varepsilon}$, while Meng defines Re = $\frac{\rho v D}{\mu}$ where D = $d\frac{\varepsilon}{1-\varepsilon}$ and d is the pebble diameter. The reported form from Dave to convert the pebble Re to the hydraulic diameter Re is flipped. Analysis in section 3 finds that the Meng correlation underpredicts Dave's data (which makes sense compared to Dave, as their Re was being multiplied by >1 and the actual Re is multiplied by <1). Dave states that in general, more porosity dependent correlations overpredict Nu ($\frac{dNu}{d\varepsilon}$ is overstated). The KTA correlation is the furthest from their results across Re, followed by Gnielinski (both overpredict), and Wakao agrees at low-moderate Re (~<1200 for FCC and ~<750 for BCC).

Dave makes an interesting claim about correlations of the form Nu = A + B$Pr^n Re^m$: "The constant n dictates the impact of the viscous to thermal boundary layer" (Dave 2019). The physical reasoning arguments will be discussed further in section 3.3.

2. **Yuan et al. (2023)[24]**: Yuan simulated the full Hermes-size reactor (Kairos Power KP-FHR) with a randomly packed core of 34,374 pebbles (4 cm diameter, ε = 0.384) using the spectral element code NekRS (wall-resolved LES). The mesh contained 60 million hexahedral elements and 7.5 billion degrees of freedom. Three FLiBe cases at Re = 160, 500, and 1,000 were simulated and Pr ranged from ~24 at inlet down to <10 when heated.

   Comparing their data against Wakao, Whitaker, Gnielinski, and KTA, they found Wakao matched best (especially in the center region), Whitaker and Gnielinski agreed within 10–20% (providing almost identical predictions), and KTA over-predicted by >20% at higher Re values.

3. **Wang et al. (2024)[15]**: Wang conducted a coupled COMSOL (electromagnetic induction heating) and ANSYS Fluent (CFD) simulation of HTS molten nitrate salt flowing

[24] Yuan et al., "High-Fidelity CFD Simulation of Mixed Convection and Forced Convection in a Pebble Bed Test Reactor Core."

through a pebble bed channel. The bed contained 16 graphite spheres to mimic and validate their prior experiments (Section 2.3, experiment 3). The study spanned Re = 2800–6600 at Pr = 11.3–14.5, ε = 0. 5685. The data reported for this analysis did not specify a specific Pr value, so Pr = 12.9 (the midpoint) is used for correlation comparison. After accounting for heat dissipation losses and gravity effects on the horizontally oriented test section (i.e. revising the fit they had to the raw data), they proposed a revised correlation:

$Nu = 5.269Re^{0.393}Pr^{0.392}$

The Wakao and KTA correlations match the data at Re ~<4200, but start to overpredict at higher Re. Wakao provides a better overall match than KTA for their data. The exact report from their work compares the correlations to their own correlation, not the raw data, so their error appears larger in this analysis than it does in the original paper. Wang does not specifically comment on Gnielinski, but from their figures it is evident that Gnielinski strongly underpredicts. The authors cite the increased momentum to thermal boundary layer ratio as the cause of the discrepancy. Since the thermal boundary layer is much smaller, the heat transfer relies on turbulent transport rather than thermal diffusion and therefore at high Re the gas correlations may overestimate the heat transfer capacity of the pebble bed.

4. **Liu et al. (2025)[8]**: Liu performed a CFD simulation of high Pr fluoride salt in a BCC pebble bed channel (D_{bed} = 9.9 mm) using FLUENT with the Delayed Detached Eddy Simulation (DDES) hybrid RANS-LES model. The study spanned Re = 50–600 (covering laminar, transitional, and turbulent regimes), Pr = 12-19, ε = 0.32 (BCC lattice). The simulation used ~6.87 million polyhedral/hexahedral cells with refined gap meshing and applied constant heat flux boundary conditions. Liu identified two critical Re values: Re = 100 (laminar-to-transitional) and 180 (transitional-to-turbulent). Existing correlations deviated significantly at low Re; comparison against KTA, Wakao, and Liu et al. (2018) Liu developed a new piecewise Nu correlation:

   The authors report that the Wakao prediction underpredicts by 34-44%. The KTA correlation matches well at Re>200 but reaches a maximum error of 26% at Re = 100 (the correlation is below the data). They explain the low Re gap between their experimental data and simulation data with experimental error being a possible factor at low Re in the physical experiment. The authors provide reasoning on the physical basis for the difference in the Wakao correlation and data by citing that the Wakao correlation was developed for Pr≈0.7 and therefore the change in ratio between momentum and thermal boundary layers at higher Pr would lead to the difference.

$$\text{Nu} = \frac{0.56}{\varepsilon^{1.043}} \text{Re}^{0.664}\text{Pr}^{0.25} \quad 180 < \text{Re} \leq 600$$

$$\text{Nu} = \frac{0.09}{\varepsilon^{0.675}} \text{Re}^{1.1}\text{Pr}^{0.25} \quad 50 \leq \text{Re} \leq 180$$

Experiment	Fluid	Re	Pr	ε	d_p	Code	Correlation
Dave (2020)	FLiBe	100-2250	16	0.26 (FCC) 0.32 (BCC)	-	STAR-CCM+	-
Yuan (2023)	FLiBe	160, 500, 1000	<10-24	0.384	40mm	NekRS	-
Wang (2024)	HTS	2800-6600	11.3-14.5	0.5685	60mm	COMSOL and ANSYS	$\text{Nu} = 5.269\text{Re}^{0.393}\text{Pr}^{0.392}$
Liu (2025)	FLiBe	50–600	12-19	0.32	9.9mm	FLUENT	$\text{Nu} = \frac{0.56}{\varepsilon^{1.043}} \text{Re}^{0.664}\text{Pr}^{0.25}$ $180 < \text{Re} \leq 600$ $\text{Nu} = \frac{0.09}{\varepsilon^{0.675}} \text{Re}^{1.1}\text{Pr}^{0.25}$ $50 \leq \text{Re} \leq 180$

Table 5: Summary of the 4 CFD experiments

2.5 All Datasets Combined Visualization

All the datasets together span a wide range across porosity, Re, and Pr ranges. To help reduce the effects of porosity and Pr range across the datasets, we provide visualizations of the data in both a pebble diameter basis (X_d) and a hydraulic diameter basis (X_h) in Figure 2. A Pr number collapse view is also provided. The standard conversion applied to the datasets and correlations is as follows (used explicitly by Liu 2018, 2025, and Wang 2022, 2024):

$$Re_h = \frac{Re_d}{(1-\varepsilon)}$$

$$Nu_h = \frac{\varepsilon Nu_d}{(1-\varepsilon)}$$

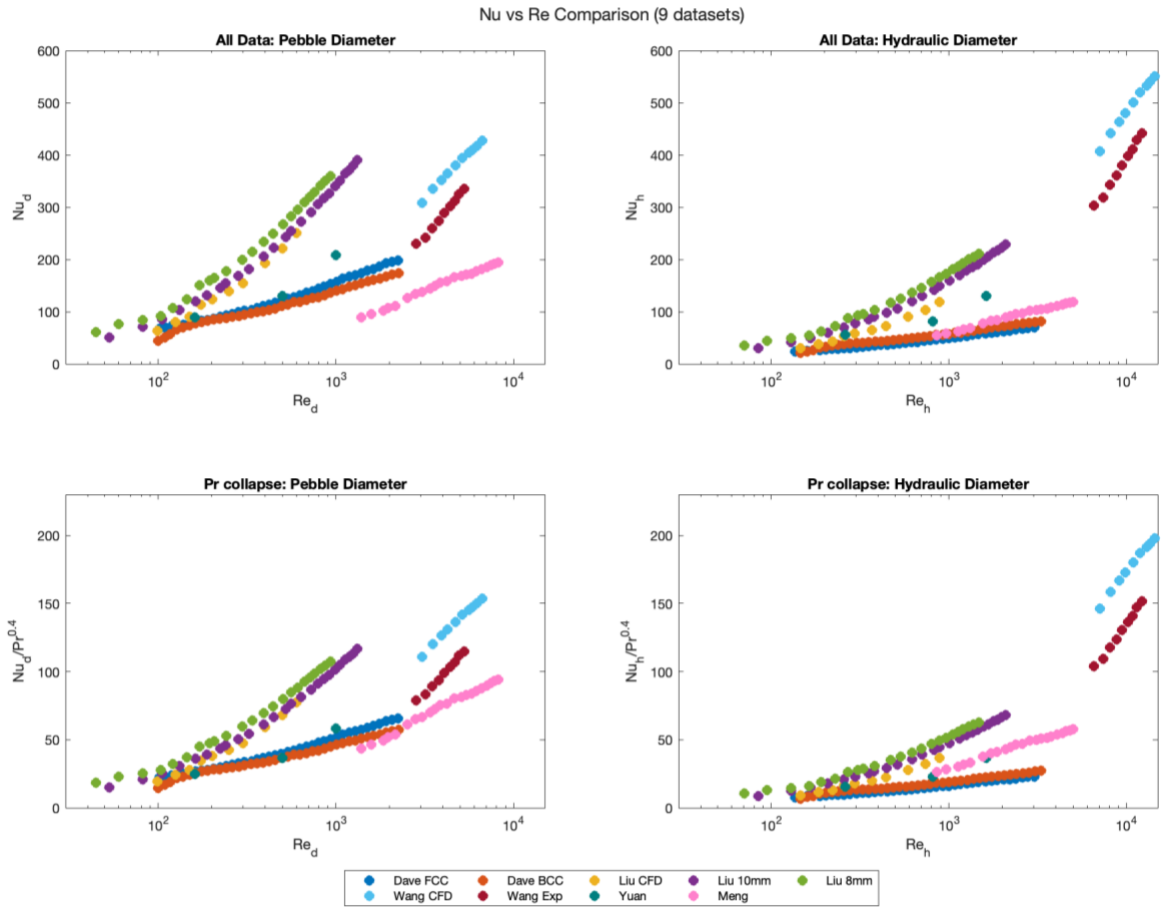

Figure 2: Visualization of the Re vs Nu plots of all 9 datasets used in subsequent analysis

As can be seen in the bottom right of Figure 2 (view that isolates the Pr and porosity spread the most), the Wang datasets are outliers in both the Re range they represent, and their porosity.

3. Evaluation of Existing Correlations

3.1 Error Across Datasets and Correlations

Each dataset (9 total, since Liu's experimental and Dave's have two relevant results per study) is quantitatively evaluated against each correlation to determine the performance of correlations across existing datasets. This serves to validate the authors' results, provide insight into the performance of newly developed correlations, and compare datasets with classic correlations that the authors did not address in their original work. Note that the Liu Experimental correlation was omitted for excessive errors (over 1000%) across some of the datasets. That high error can likely

be attributed to the ε^4 term in the denominator that greatly exaggerates the effect porosity has on the Nu value.

The correlations are assessed at the reported Re, Pr, and ε of each dataset. In some cases, Pr is provided as a range, not a single value. In this case, the Pr value that provided results closest to the authors' published data (i.e. visually how the data compares against existing correlations) was used. Re_h and Re_d were extracted for each dataset. The data was recorded in the basis that the paper specified, and then converted to the other one using the convention established in Section 2.5. Error is evaluated using the Mean Absolute Relative Error (MARE) convention. The porosity and Pr scaling applied in section 2.5 translates the curve across the Re-Nu space, but it does not transform the shape of the curves nor the error between the data and correlations. The following data is presented in only the Re_d view since that accurately represents the performance of correlations at each dataset.

The wide range of datasets and their spread across Re, porosity, and Pr all contribute to inconsistencies across the results and how well correlations can predict their performance. This evaluation and subsequent analysis acknowledge that all these factors contribute to performance differences and must all be considered in evaluations. Since the correlations are evaluated at a wide range of Re across all the datasets, there are at least a few datasets that sit in their range of validity, and therefore give a fair evaluation (at least in terms of their Re value). This is not to say that extrapolating beyond the Re range does not cause errors, because it may, but it is likely not the leading cause for the performance spread across the 9 datasets. The Pr spread across the datasets is generally contained in the 12-19 range, which does represent a large spread but still within the same order of magnitude. The Meng experiment with water is the exception to this. Additionally, the Pr range is an order of magnitude (water) or two (molten salt) higher than what many of the correlations are intended for, so this is a known uncertainty that is somewhat shared across the datasets. The porosity range of validity on many correlations is more limited and is less discussed as a factor causing disagreements between data and correlations than Pr is. To investigate this further, subsequent figures are visually organized by porosity to convey any dependence this factor may have on the correlation's performance.

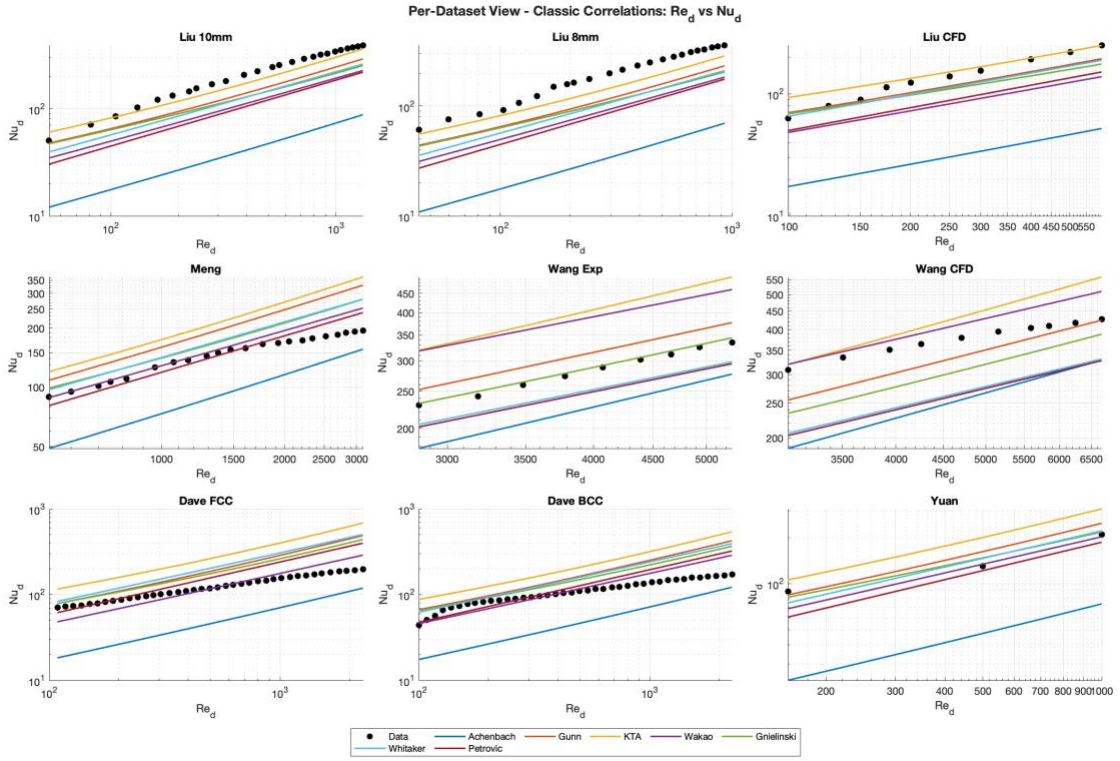

Figure 3: Performance of the 7 classic correlations against each dataset

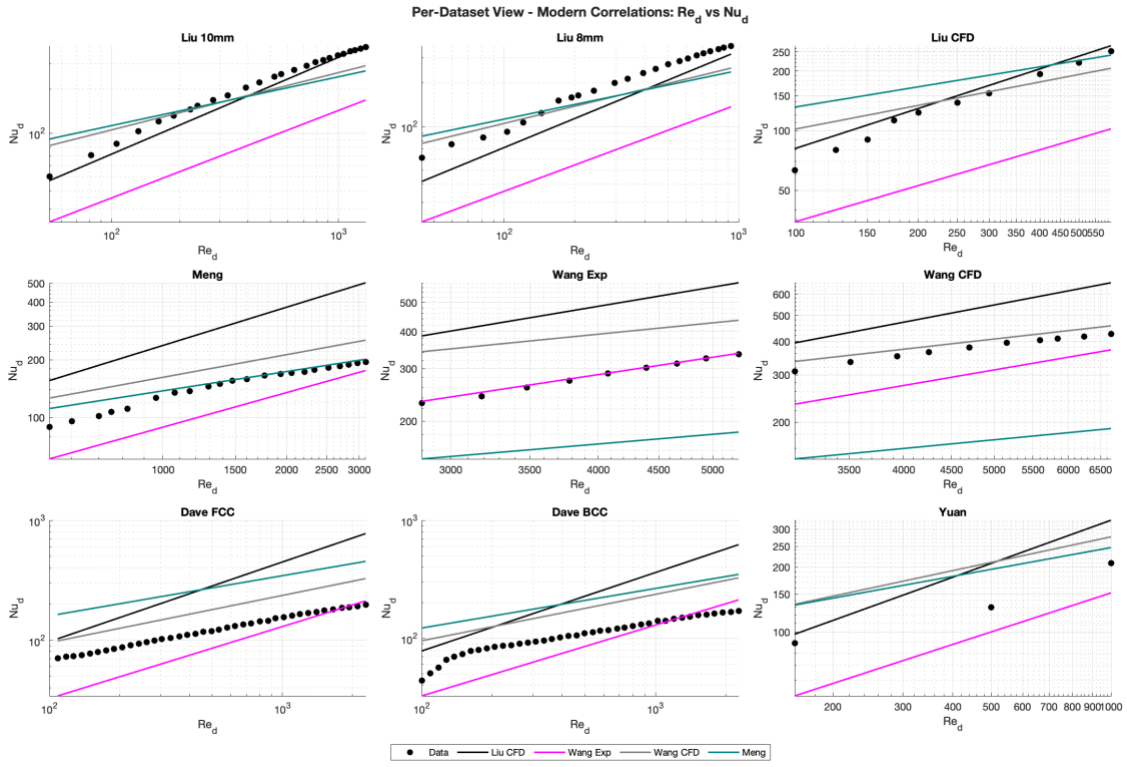

Figure 4: Performance of the 4 modern correlations against each dataset

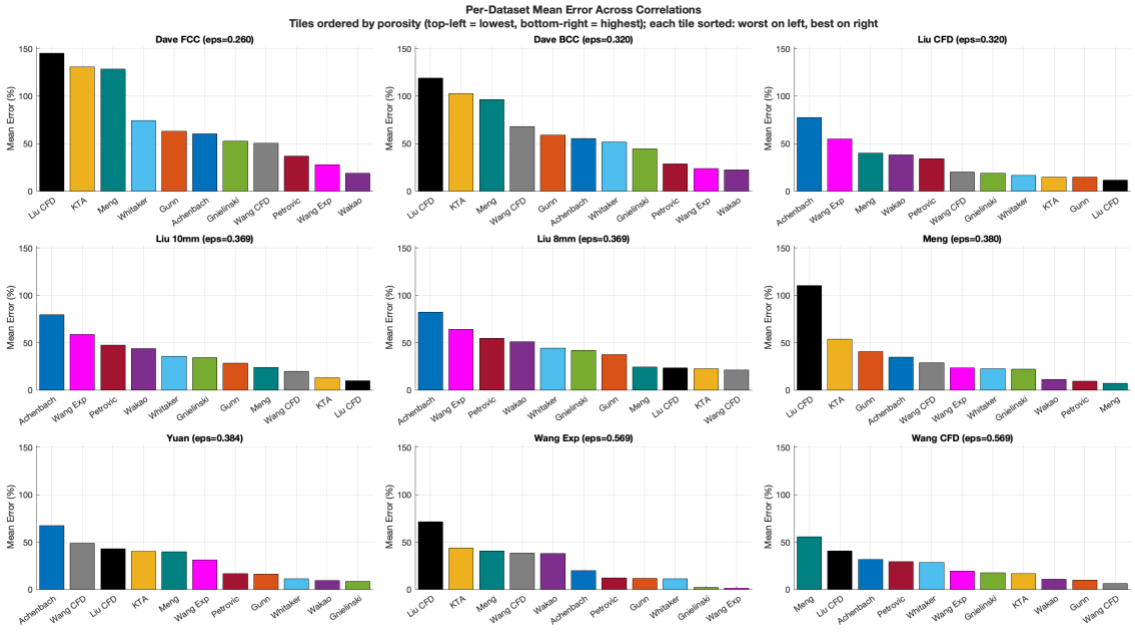

Figure 5: Performance of each correlation on each dataset. The tiles are organized in porosity order (lowest porosity top left and highest bottom right), and within each tile the errors are ordered from most (left) to least (right)

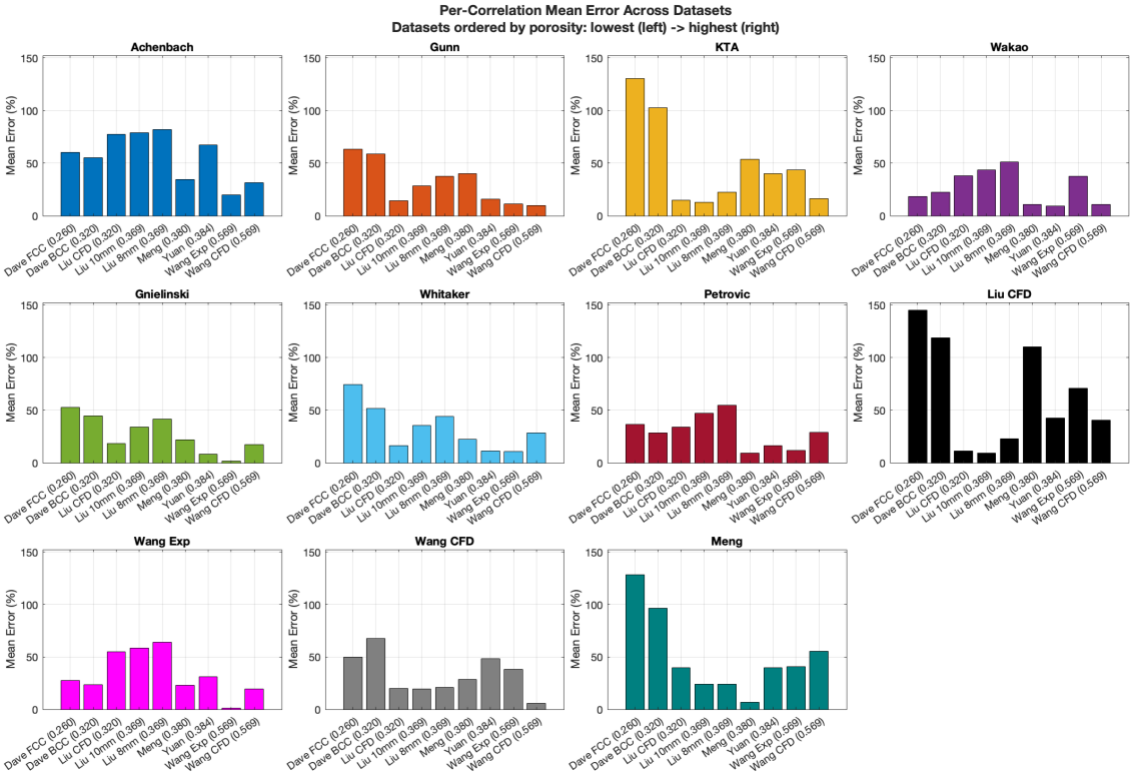

Figure 6: Performance each correlation at all datasets (same information presented as figure 5, but visualized differently). The datasets along each x-axis are organized by porosity (left = lowest porosity, right = highest porosity).

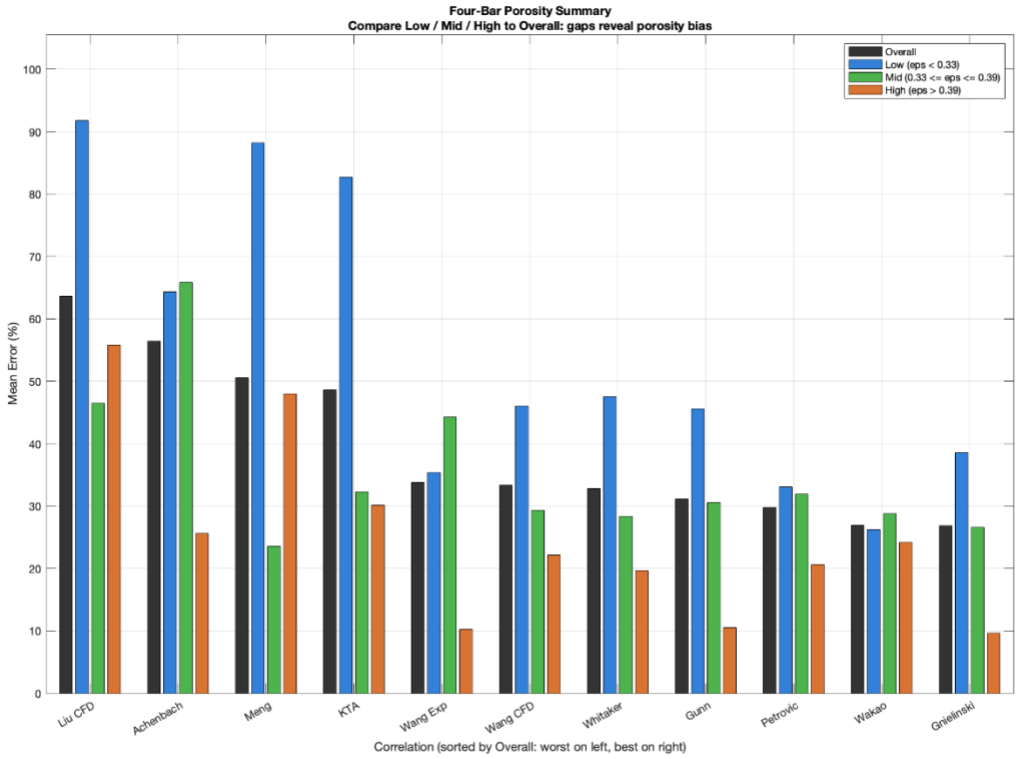

Figure 7: Performance of each correlation evaluated at the different porosity ranges. Black bars represent the total mean error across all datasets, blue are datasets with porosity <0.32, orange are datasets with porosity >0.39, and green represents the remaining datasets

3.2 Summary of performance

Achenbach: Consistently underpredicts the Nu value across all the datasets. This is to be expected, as it lacks a Pr term in the equation and was created for gases where Pr = 0.7, so when scaled up to an order of magnitude higher Pr, it is unable to capture the increased heat transfer capabilities that the thinner thermal boundary layer can create.

Gunn: Performs the worst at low porosities, and very well at high porosities. Gunn overpredicts all the Liu datasets as well as Wang CFD, and underpredicts the rest. Its porosity-based bias may be attributed to the quadratic porosity terms embedded in the correlations.

KTA: Greatly overpredicts at low porosities and improves performance as porosity increases. The Liu datasets are an exception to that trend, exhibiting the lowest error despite being in the low to mid porosity. This may be due to the Liu datasets rather than something attributed to the KTA behavior. The Liu datasets are underpredicted by every correlation, whereas the other datasets generally sit somewhere in the middle (i.e., some over predict while some under

predict). While this may be attributed to the low Re range, the fact that both Dave datasets and Yuan say KTA overpredicts while Liu underpredicts is cause to keep the general KTA trend across porosity argument and omit Liu from the overall trend explanation. KTA is discussed in the literature as well: Dave claims KTA is overly sensitive to ε increases, Wang discusses their high ε driving the KTA increase, and Liu claims KTA's success at lower Re values comes from the fact that ε strongly influences behavior. KTA being highly porosity dependent is evident from the literature and the trend presented in Figure 6, and therefore should be a key consideration when using the KTA correlation.

Wakao: Exhibits more consistent error behavior across the porosity ranges, which may be attributed to its lack of an explicit porosity dependence in the equation. Wakao was correlated for ε = 0.4, so it should follow that lower ε values = denser packed beds = better heat transfer than Wakao, and higher ε values = sparser beds = lower HT than Wakao. Liu and Dave's datasets are on the lower porosity side and are overpredicted by Wakao, and Wang's datasets are on the higher porosity side and are underpredicted by Wakao. These trends support this line of reasoning, aiming to explain why Wakao may over/underpredict.

Gnielinski: Prediction performance (absolute error) generally improves as porosity increases. Excluding the Liu datasets (same reasoning as the KTA section above), the Gnielinski correlation tends to overpredict at low porosities and match/underpredict at higher porosities. The porosity dependence embedded in the equation may exaggerate the impact that porosity has on the Nu values.

Whitaker: Performs better at higher porosities, as anticipated in his own work. The author claims that regular arrangements (as opposed to random) will be better predicted by his correlation, and beds with higher porosities represent a more orderly arrangement than a random bed.

Petrovic: Exhibits generally even behavior across the varying porosities, with the highest errors in the low porosity range, closely followed by errors in the mid-range.

Liu CFD: Exhibits the highest error across the porosity spectrum, with particularly high errors at the low porosity range. This correlation has a $\varepsilon^{0.675}$ term in the denominator that may be artificially inflating the Nu values at low porosities. This correlation greatly overpredicts at all porosity ranges except its own datasets, so it is likely that the porosity term in the denominator is skewing the values artificially high.

Wang Exp: Performs well at the two porosity extremes but exhibits higher error in the middle. It underpredicts the Nu value of all the datasets, except Dave at the high Re end. This result is interesting because Wang is the highest porosity, but it works well on the lower end and worse in the middle range. It may be that it does encode porosity dependence well, but only at the extremes.

Wang CFD: Exhibits the inverse trend of its experimental counterpart and performs worse at the porosity extremes than at the intermediate porosity values (except for its comparison to its own

data). The CFD data sits higher than the experimental data does, so the correlation follows a similar trend as the experimental one, but shifted upwards, which moves it above the Nu values of some of the datasets and below others. The experimental datapoints were fairly low compared to the other datasets, so this change in performance can be attributed to the change in datasets the correlation is based on.

Meng: Performs well in the mid porosity range and worse at the extremes. Overpredicts at lower porosities and underpredicts at higher porosities. The lack of a specific porosity dependence can explain this behavior.

General summary: Correlations generally tend to perform worse at the low porosities and show mixed results at the mid and higher porosities. The overall best performing correlations at the different porosities are as follows: Gnielinski is best for high, Meng is best for mid-range, Petrovic is best at low porosities, and Wakao demonstrates the most consistency across the different porosities.

3.3 Single Sphere OpenFOAM Study

3.3.1 Boundary Layer Argument

The driving factor behind the studies presented above and a leading theory for why the existing correlations may not map well to the case of molten salt is the increased Pr. By definition, increasing Pr means that the ratio between the momentum and thermal viscous boundary layer also increases. Many papers point towards this shifting ratio as the underlying physical cause of the errors in Nu number predictions from gas to molten salt applications.

Dave (2018) claims that due to the smaller relative thermal boundary layer, "heat transport to FliBe is dominated by turbulent mixing at the boundary layer rather than thermal molecular diffusion". In a later paper, Wang offers a similar explanation to Dave (2018), pointing towards turbulence rather than general momentum: "heat transfer between the fluid and the pebble mainly relies on turbulent transport rather than thermal diffusion" (Wang 2024). Liu points towards a difference in the convective heat transfer mechanism at differing Pr values: "with Pr = 14–19, the fluid thermal boundary layer is much thinner, indicating that the heat transfer is dominated by the momentum diffusivity at the boundary layer" (Liu 2018). Liu's subsequent CFD study offers a more rigorous quantitative explanation of the same phenomena. They define α = molecular diffusivity, $\alpha_t = \frac{\upsilon_t}{Pr_t} = \frac{\text{turbulent eddy viscosity}}{\text{turbulent Prandtl number}}$ = turbulent thermal diffusivity, and $\alpha_{eff} = \alpha + \alpha_t$ = effective diffusivity (sum of thermal and turbulent thermal diffusivities). From this, they conclude: "this $[\frac{\alpha}{\alpha_{eff}}]$ ratio exceeds 60 % for water. In contrast, for fluoride salt, the ratio remains below 25 %, confirming that turbulent thermal diffusion plays a significantly larger role in heat transfer due to its high Prandtl number" (Liu 2025).

Every author makes the argument that the thermal molecular boundary layer becoming much thinner than the momentum molecular boundary layer shifts heat transport away from molecular thermal diffusion. Dave, Wang, and Liu 2025 specifically point towards turbulence, while Liu 2018 makes a more general claim about momentum diffusivity in general. It is important to note that FHR operating ranges tend to be 100-1000 (Dave 2019), so that does not necessarily qualify as turbulence, but more in a transition state towards turbulence. The general momentum effect is a more conservative explanation and more applicable to the laminar or quasi-laminar regime. In summary, as the flow starts to leave the laminar regime and transitions towards turbulence (e.g., periodic boundary layer detachments, aperiodic eddying, and other transitions), the effective Pr number becomes smaller than the molecular Pr, indicating that the effective thermal and momentum boundary layer thicknesses become closer to each other. If the rest of the correlations remain valid (which is an approximation), this would indicate that the Nu number correlation dependence on the laminar Pr number would overpredict the effective Nu. Of course, in these cases, the whole correlation may need to be updated to account for the different transition regimes and configurations of the pebble beds. Such modification of the correlation parameterizations may then lead to differing dependence on the molecular Pr and effective Pr.

3.3.2 OpenFOAM Study

To validate the change in boundary layer ratio across the different fluids and provide a porosity-independent datapoint to compare the (single sphere) Whitaker correlation to, a supplementary study was performed using OpenFOAM. The Whitaker correlation for a single sphere is defined as $Nu = 2 + (0.4Re^{1/2}+0.06Re^{2/3})Pr^{0.4}$ (Whitaker 1972). Note that this is not a direct comparison to the packed bed case, but it can still provide useful insight into how the correlation predictive power changes with changing Re and Pr.

An isolated heated sphere (D = 10cm) was modeled in laminar cross flow. Constant heat flux q" = 48.5 $\frac{kW}{\mathrm{m2}}$ was applied (this value is taken as it was the time-averaged heat flux value provided in the Kairos documentation (Source)). The three fluids evaluated were air at 550K (Pr = 0.7), water at 300K (Pr = 6.87), and FLiBe at 873K (Pr = 20.4). Three different Re number cases were evaluated (Re = 160, 500, 1000) to both span the relevant Re range in molten salt PBRs (100-1000) and match the three Re values evaluated by Yuan. The evaluated fluids have the properties listed in Table 6.

	Air	Water	FliBe
Inlet Temp [K]	550	300	873
ρ [$\frac{kg}{m^3}$]	0.64	997	1987
C_p [$\frac{J}{kgK}$]	1040	4180	2398
k [$\frac{W}{mK}$]	0.043	0.607	1.0
μ [Pa·s]	2.88e-5	1e-3	8.5e-3

Pr [-]	0.7	6.87	20.4

Table 6: Thermophysical property values used in the OpenFOAM study

The study was performed using the incompressibleFluid solver module with steady state SIMPLE. No turbulence model was used; the simulations were set to simulationType laminar in OpenFOAM. The Re range studied is 160–1000, which is well below the laminar-to-turbulent boundary-layer transition on a sphere ($Re \approx 2 \times 10^5$). Temperature was solved as a passive scalar via scalarTransport. Wall heat flux was imposed using fixedGradient and the mesh was 192k cells (blockMesh + snappyHexMesh). A finer grid was used on the Re = 1000 case (due to thinner boundary layer) with 647k cells.

The boundary layer scaling followed the theory, with the momentum boundary layer remaining the same across the fluids (by design, since it was based only on Re) and the thermal boundary layer thinning with increasing Pr. Figure 8 shows a visualization of the two boundary layers, and Figure 9 plots the boundary layer thickness from 30-130°. Note that the steady-state solution has not yet been reached, hence the eddying behavior, even though we solve for the mean flow.

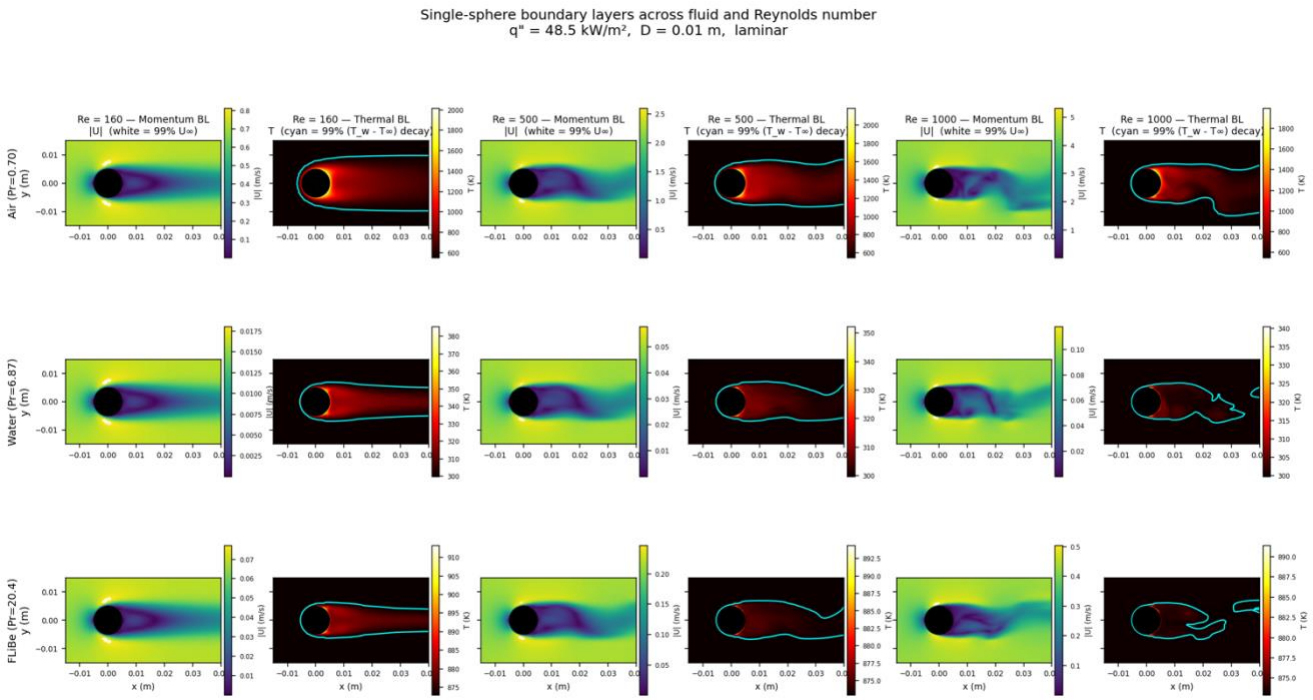

Figure 8: Visualization of the momentum (1st and 3rd columns) and thermal (2nd and 4th columns) boundary layers at the Re = 160 case (1st and 2nd columns) and the Re = 1000 case (3rd and 4th columns).

Nusselt number summary: CFD vs Whitaker correlation
Single sphere, q" = 48.5 kW/m², D = 0.01 m, laminar

Fluid	Re	Pr	T_wall (K)	ΔT (K)	h (W/m²K)	Nu (CFD)	Nu (Whitaker)	rel error
Air	160	0.70	1958	1408	34	8.01	7.91	**+1.3%**
Water	160	6.87	349	49	990	16.31	16.76	**-2.6%**
FLiBe	160	20.38	894	21	2343	23.43	24.81	**-5.6%**
Air	500	0.70	1472	922	53	12.24	13.01	**-5.9%**
Water	500	6.87	329	29	1662	27.38	29.50	**-7.2%**
FLiBe	500	20.38	885	12	4079	40.79	44.50	**-8.3%**
Air	1000	0.70	1262	712	68	15.85	18.14	**-12.6%**
Water	1000	6.87	322	22	2198	36.21	42.30	**-14.4%**
FLiBe	1000	20.38	882	9	5375	53.74	64.28	**-16.4%**

Whitaker over-predicts CFD (negative rel error) Whitaker under-predicts CFD (positive rel error)

Figure 9: Results of the OpenFOAM simulations: computed Nu value, ΔT, and computed relative error

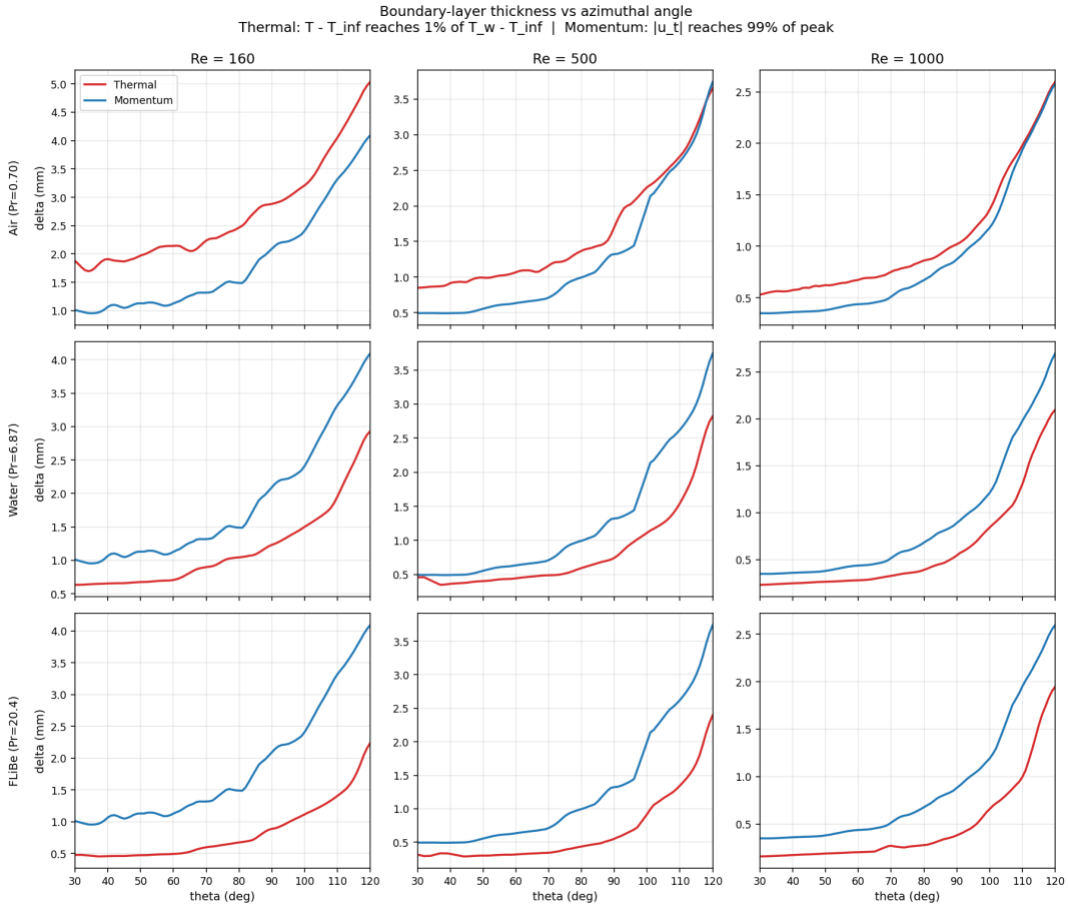

Figure 10: Boundary layer thickness at the varying fluids and Re values. Red represents the thermal boundary layer and blue the momentum boundary layer.

The thickness of the BLs is represented in Figure 10. The thermal BL thins by ~$Re^{-1/2}$ and by ~$Pr^{0.33-0.4}$, values which are reflected in Whitaker's single sphere correlation and in other correlations presented in Section 2.

The study is benchmarked against the Whitaker correlation to assess performance. Results are presented in Figure 9. There is not a clear argument to be made from the results presented in Figure 9 that the correlation works well for air and not for FLiBe. The error is of a similar magnitude across the fluids at the Re = 500 and 1000 cases, and the error scales more with Re than with Pr. From this result, the boundary layer argument is not necessarily the leading cause of discrepancies at the Re = 500 and 1000 cases, since performance is only minimally worse at the higher Pr cases. It should also be noted that Whitaker states that expected errors should fall within 15% of predicted values, so all values except FLiBe at Re = 1000 predicted by the study fall within the acceptable error range, and speculating within this range may be going beyond what the correlation is validated to do.

Another observation that should be noted from Figure 9 is the required ΔT to achieve the set heat flux. The wall temperature and ΔT for air is an order of magnitude higher than for the water and FLiBe cases across all the Re values, and is particularly pronounced at the Re = 160 case. The ΔT represented here is physically unrealistic and would require a sphere temperature well beyond what the TRISO particles would be able to physically handle. This value underscores the motivation to pursue molten salt as the working fluid in the first place: it is far more effective at transferring heat than gases. The required ΔT is fairly similar to water, but FLiBe can operate at higher temperatures and lower pressures than water, leading to higher efficiency and improved safety.

4. New Fit method and validation

4.1 Method for fit and validation

To improve upon the existing set of available correlations, a new correlation was fit to the datasets discussed. The purpose of this is to create a correlation based on aggregated data specifically at high Pr datasets (i.e., not including gases) to supplement the gap in the current literature. A similar methodology was applied in another study (Wu 2025), but was done on aggregated data across the full Pr spectrum and included geometry-specific terms that did not apply to many datasets discussed above (the studies did not always provide full geometric details beyond pebble diameter).

Based on the results from section 3.2, the highest performing correlations were Gnielinski, Meng, Petrovic, and Wakao. The latter three have the following canonical forms: $Nu_h =$

$ARe_h{}^b Pr^c$, $Nu_d = \frac{ARe_d{}^b Pr^c}{\varepsilon}$, and $Nu_d = A + DRe_d{}^b Pr^c$ (respectively). Given that these each follow the general form of Nu = $ARe^b Pr^c$, this functional form was used as the structure and exponents were fit based on the datasets. The A + term in Wakao was dropped because at the Re values most relevant to the reactor (100-1000) the +2 inclusion becomes less relevant, and the ε term from Petrovic was dropped because of the general inconsistency of porosity-dependent functions across the datasets, as discussed in section 3.2. The Gnielinski form was too complex to try and recover from a curve fitting approach.

To find the optimal exponents, three parameters were varied. In finding the exponents, the c term was fixed in the typical range found across the literature (generally $\frac{1}{3}$ to 0.45) to ground the correlation in the physical Pr scaling argument presented in Figure 10. Four different combinations of datasets to evaluate against were tried. The options were to keep all 9 datasets, drop both Wang datasets, drop both Dave datasets, or drop both Wang and Dave. This was chosen because Dave is a porosity outlier, and Wang is a porosity and Re range outlier (seen in Figure 2). Finally, the fits were evaluated on both the hydraulic diameter basis and the pebble diameter basis to account for how including porosity variations might affect the fit.

Every permutation of the above factors was tested by performing an ordinary least squares linear regression in log space to fit a power law to the general form Nu = $ARe^b Pr^c$ and using MATLAB's fit() function to find the optimal coefficients. With values computed at each of the permutations above, optimal fit was determined by computing the mean error across all datasets with the proposed coefficients and ranking them from least to most. The top 6 best performing combinations were all using pebble basis, and dropping both Wang, with performance falling as the c value decreased from c = 0.4 to c = 0.392.

The optimal correlation from this search is defined as:

Nu = $4.08Re^{0.39}Pr^{0.4}$

4.2 Comparing New Fit Error with Other Correlations

The new fit is compared against the top performing correlations from Section 3 in the direct data point evaluation, and against all the correlations in the remaining visualization figures.

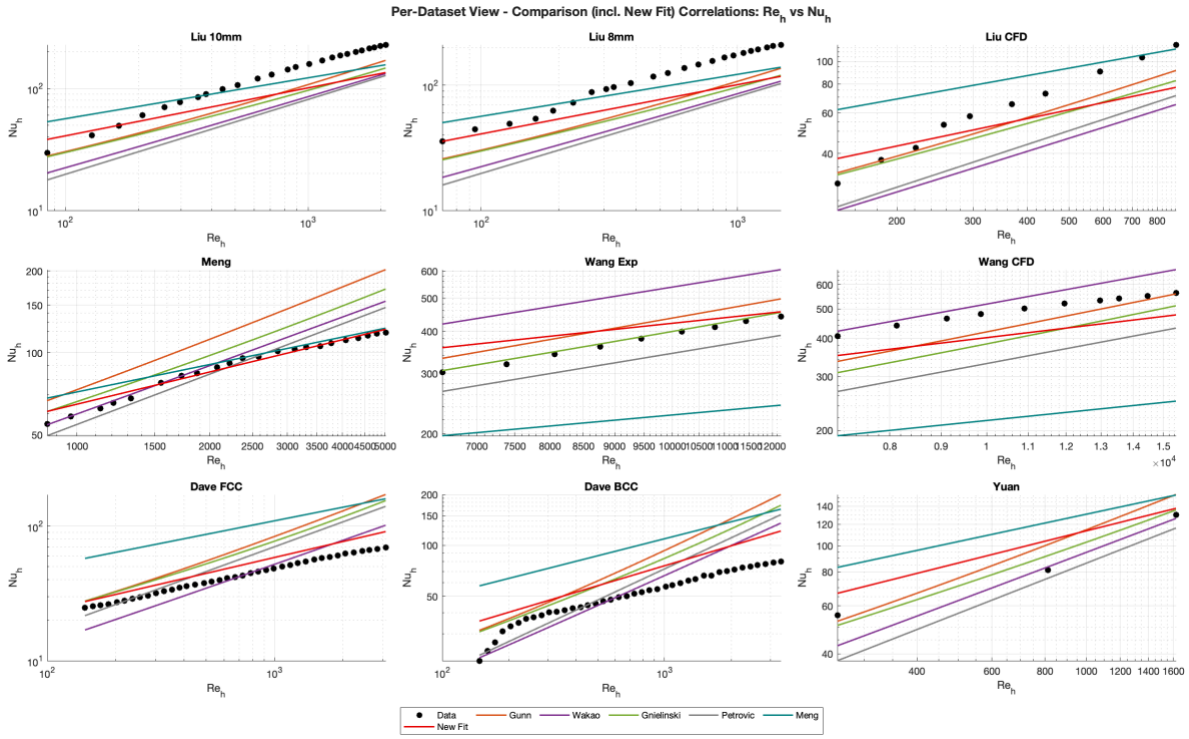

Figure 11: Performance of the new fit against the top 5 performing current correlations

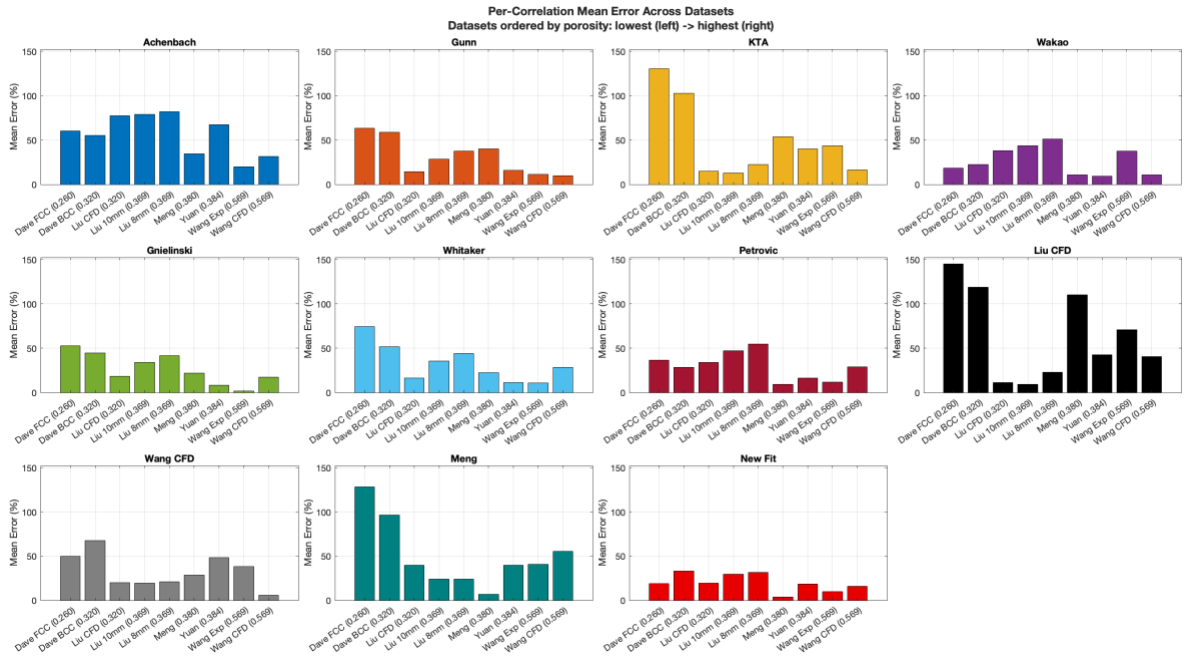

Figure 12: Performance of each correlation on each dataset, with new fit included. The tiles are organized in porosity order (lowest porosity top left and highest bottom right), and within each tile the errors are ordered from most (left) to least (right).

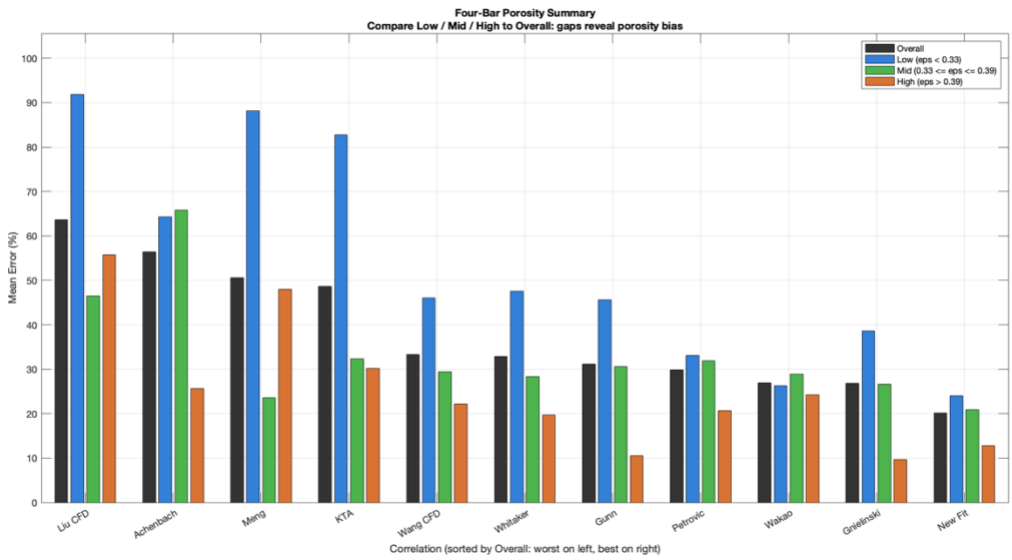

Figure 13: Performance each correlation evaluated at the different porosity ranges. Black bars represent the total mean error across all datasets, blue are datasets with porosity <0.32, orange are datasets with porosity >0.39, and green represents the remaining datasets.

4.3 Improvements

The new correlation performs fairly consistently across the porosity ranges (not as consistently as Wakao) and has the lowest error in the mid and low porosity ranges. Since the mid-porosity range is the most relevant to FHR conditions, being lower in that region is most significant for improving accuracy in a real-life use case. The primary reason for the improved fit is that it was trained on this data (minus Wang) more than any physically grounded reasoning for the exponents. This was affirmed with a leave one out validation check, and the mean errors were similar except for the Dave datasets (which is to be expected, since these are at the porosity outliers of the higher Pr exponent (0.4 vs $\frac{1}{3}$) is supported by both Meng and Wang, who have higher Pr exponents when using a higher Pr fluid to help capture the theoretical improved heat transfer that fluids offer over gasses. The Pr exponent of 0.4 aligns with empirical practice for high-Pr fluids (previously stated authors, as well as the standard Dittus-Boelter correlation), but the OpenFOAM study in Section 3.3 suggests the boundary-layer-ratio argument is perhaps not the single or dominant error source at moderate Re. The improved Pr exponent is empirically calibrated, not necessarily derived from the boundary-layer mechanism, as some of the literature discussed in section 3.3.1. The Re exponent of 0.39 fits the Re range of 100–1000, which is smaller than the $Re^{0.6–0.7}$ exponents in Wakao and Gunn that were calibrated in higher-Re gas-cooled beds. The lack of porosity dependence also helps to avoid high errors at the porosity extremes, something that correlations with an encoded porosity dependence may experience.

5. Conclusion

5.1 Summary

This thesis addressed a gap in pebble-bed Nu number correlations for FHR conditions, where Pr (Pr ≈ 11–25) and Re numbers (≈ 100–1000) fall well outside the gas-cooled (Pr ≈ 0.7, Re ~ O(10^5)) regimes on which classic correlations were developed. A consolidated high Pr dataset was compiled from three experimental studies (Meng, Liu, Wang) and four CFD studies (Dave, Yuan, Wang, Liu) with porosities ranging from 0.26–0.57. Seven classical correlations (Whitaker, Gunn, Wakao, KTA, Achenbach, Gnielinski, Petrovic) and four modern high-Pr correlations (Liu CFD, Wang experimental, Wang CFD, Meng) were benchmarked against this combined dataset using mean absolute relative error, with results stratified by porosity bin to illuminate porosity-dependent biases.

KTA, Gnielinski, and Gunn over-predicted strongly at low porosities and improved at higher porosities, a behavior attributable to their explicit ε-dependent terms being extrapolated outside their intended ranges. Achenbach consistently under-predicted all datasets, consistent with its lack of a Pr term. Wakao demonstrated the most consistent behavior across porosities, and no single correlation performed exceptionally well across all conditions. A supplementary OpenFOAM single-sphere study was performed to address the commonly cited boundary-layer-thinning argument for explaining gas-versus-salt discrepancies. The study found that the argument does not solely explain the behavior of laminar single-sphere geometries (which did not show drastic Nu differences at different Pr values). This result suggests that packed-bed-specific transport mechanisms, in addition to pure boundary-layer scaling, may be driving the observed errors.

A new correlation of the form $Nu = 4.08 \cdot Re^{0.39} Pr^{0.4}$ was developed via ordinary least-squares regression in log-space across a subset of the compiled data (everything except the Wang datasets). This fit achieved the lowest mean error in the low and mid porosity bins (the regime most relevant to FHR operation) compared with the other 11 correlations. The exponents are consistent with the mid-range Re scaling and high-Pr empirical practice observed across other independent fits in the literature.

5.2 Limitations

The compiled dataset aimed to span relevant conditions, but it only contains 9 datasets across 7 studies. Most lie in the mid porosity ranges, so the two extreme cases (Wang and Dave) are not confirmed by other independent datasets. The proposed correlation does not contain an explicit porosity term and therefore cannot represent any porosity physics occurring in the actual reactor. The consistent performance across ε is due to empirical averaging rather than mechanistic

accuracy. The fit is calibrated within Re ≈ 50–6600 and Pr ≈ 6–24, so extrapolation outside this range would not be explicitly supported by this study. The dataset also carries the uncertainties (measurement error, turbulence model selection, mesh resolution for CFD, etc) embedded in the original studies. Also, the functional form of the correlations may need to adapt to the Re and effective Pr numbers and account for different quasi-turbulent regimes as well as parameters describing the pebble configurations.

5.3 Future Work

Three future directions are proposed to strengthen the analysis presented in this thesis. First, additional high-Pr experimental data, particularly at low porosity ($\varepsilon < 0.35$) and across a broader Re range, would reduce uncertainty induced by individual datasets representing entire porosity bins. Second, an expansion from the single-sphere study to a dedicated packed-bed CFD study focused on the pebble-fluid interface dynamics (as opposed to full core simulations) would help resolve whether turbulent transport, momentum diffusion, or something else is driving the high-Pr discrepancy. Third, incorporating an explicit, physically motivated porosity term (rather than the empirically fit ε-dependencies of existing correlations) could strengthen the validity of the proposed correlation at the porosity extremes. Each of these directions would help with grounding existing or improved correlations in physical reality, instead of relying mostly on empirical correlations or limited experimental observations.

Bibliography

"Achenbach- Heat and Flow Characteristics of Packed Beds." n.d.

Dave, A. J., K. Sun, and L. Hu. "Numerical Assessment of Packed-Bed Heat Transfer Correlations for Molten Salt." *Annals of Nuclear Energy* 136 (February 2020): 107002. https://doi.org/10.1016/j.anucene.2019.107002.

Energy.Gov. "X-Energy Is Developing a Pebble Bed Reactor That They Say Can't Melt Down." May 8, 2026. https://www.energy.gov/ne/articles/x-energy-developing-pebble-bed-reactor-they-say-cant-melt-down.

"Generation IV Goals, Technologies and GIF R&D Roadmap | GIF Portal." Accessed May 11, 2026. https://www.gen-4.org/generation-iv-criteria-and-technologies.

"Generation IV Nuclear Reactors - World Nuclear Association." Accessed May 11, 2026. https://world-nuclear.org/information-library/nuclear-power-reactors/other/generation-iv-nuclear-reactors.

Gunn, D. J. "Transfer of Heat or Mass to Particles in Fixed and Fluidised Beds." *International Journal of Heat and Mass Transfer* 21, no. 4 (1978): 467–76. https://doi.org/10.1016/0017-9310(78)90080-7.

Hu, Guojun, Daniel O'Grady, Ling Zou, and Rui Hu. *Development of a Reference Model for Molten-Salt-Cooled Pebble-Bed Reactor Using SAM*. ANL/NSE--20/31, 1674975, 162241. 2020. https://doi.org/10.2172/1674975.

IAEA. "Data Centres, Artificial Intelligence and Cryptocurrencies Eye Advanced Nuclear to Meet Growing Power Needs." Text. December 4, 2024. http://www.iaea.org/bulletin/data-centres-artificial-intelligence-and-cryptocurrencies-eye-advanced-nuclear-to-meet-growing-power-needs.

Khan, Zahra. "Approval of Nuclear Pilot Plant That Uses Molten Salt Coolant Instead of Water a Step towards Safer Reactors." Chemistry World. Accessed May 11, 2026. https://www.chemistryworld.com/news/approval-of-nuclear-pilot-plant-that-uses-molten-salt-coolant-instead-of-water-a-step-towards-safer-reactors/4018890.article.

"KP-FHR Core Design and Analysis Methodology Topical Report." https://www.nrc.gov/docs/ML2409/ML24095A258.pdf

KTA 3102.2 Reactor Core Design of High-Temperature Gas-Cooled Reactors; Part 2: Heat Transfer in Spherical Fuel Elements. n.d.

Liu, Limin, Dalin Zhang, Linfeng Li, et al. "Experimental Investigation of Flow and Convective Heat Transfer on a High-Prandtl-Number Fluid through the Nuclear Reactor Pebble Bed Core." *Applied Thermal Engineering* 145 (December 2018): 48–57. https://doi.org/10.1016/j.applthermaleng.2018.09.017.

Liu, Limin, Jiaming Zhang, Tenglong Cong, Yao Xiao, and Hanyang Gu. "Numerical Research of Flow and Heat Transfer Characteristics of High-Prandtl-Number Fluoride Salt in the Pebble Bed Channel." *Progress in Nuclear Energy* 189 (November 2025): 105936. https://doi.org/10.1016/j.pnucene.2025.105936.

Manohar S. Sohal, Matthias A. Ebner, Piyush Sabharwall, and Phil Sharpe. *Engineering Database of Liquid Salt Thermophysical and Thermochemical Properties*. INL/EXT-10-18297, 980801. 2010. https://doi.org/10.2172/980801.

Meng, Xianke, Zhongning Sun, and Guangzhan Xu. “Single-Phase Convection Heat Transfer Characteristics of Pebble-Bed Channels with Internal Heat Generation.” *Nuclear Engineering and Design* 252 (November 2012): 121–27. https://doi.org/10.1016/j.nucengdes.2012.05.041.

Ortensi, Javier, Cole Mueller, Stefano Terlizzi, Guillaume Giudicelli, and Sebastian Schunert. *Fluoride-Cooled High-Temperature Pebble-Bed Reactor Reference Plant Model*. INL/RPT--23-72727-Rev000, 1983953. 2023. https://doi.org/10.2172/1983953.

“Pronghorn Theory Manual.” https://inldigitallibrary.inl.gov/content/uploads/50/2026/04/Sort_24425.pdf

“Role of Natural Gas.” Accessed May 11, 2026. https://www.iso-ne.com/about/where-we-are-going/role-of-natural-gas.

Wakao, N. *FLUID DISPERSION COEFFICIENTS ON PARTICLE-TO-FLUID HEAT TRANSFER COEFFICIENTS IN PACKED BEDS*. n.d.

Wang, S. W., C. Zhou, C. X. Cai, H. H. Zhu, N. X. Wang, and Y. Zou. “Experimental Research on Convective Heat Transfer Characteristics of Molten Salt in a Pebble Bed Channel with Internal Heat Source.” *Nuclear Engineering and Design* 387 (February 2022): 111619. https://doi.org/10.1016/j.nucengdes.2021.111619.

Wang, S. W., C. Zhou, N. X. Wang, C. X. Cai, H. H. Zhu, and Y. Zou. “Numerical Analysis and Validation on Heat Transfer Characteristics and Correlation of Molten Salt in Pebble Bed Channel.” *Nuclear Engineering and Design* 418 (March 2024): 112920. https://doi.org/10.1016/j.nucengdes.2024.112920.

Whitaker, Stephen. “Forced Convection Heat Transfer Correlations for Flow in Pipes, Past Flat Plates, Single Cylinders, Single Spheres, and for Flow in Packed Beds and Tube Bundles.” *AIChE Journal* 18, no. 2 (1972): 361–71. https://doi.org/10.1002/aic.690180219.

Wikipedia. “Pebble-bed reactor.” April 17, 2026. https://en.wikipedia.org/w/index.php?title=Pebble-bed_reactor&oldid=1349471472.

Wu, Xiaomin, and Takashi Hibiki. “Particle-Fluid Heat Transfer for Laminar and Turbulent Flows in Packed Beds of Spherical Particles.” *International Journal of Heat and Mass Transfer* 236 (January 2025): 126257. https://doi.org/10.1016/j.ijheatmasstransfer.2024.126257.

Yuan, Haomin, Tri Nguyen, David Reger, et al. “High-Fidelity CFD Simulation of Mixed Convection and Forced Convection in a Pebble Bed Test Reactor Core.” *Nuclear Technology* 211, no. 10 (2025): 2534–58. https://doi.org/10.1080/00295450.2024.2437310.